Study on the COP of free piston Stirling cooler (FPSC) in the anti-sublimation CO2 capture process

doi: 10.1016/j.renene.2014.08.071

Study on the COP of Free Piston Stirling Cooler (FPSC) in the anti-sublimation CO_2 capture process

Chunfeng Song [a, *], Jingwen Lu [b], Yutaka Kitamura [b]

[a] *School of Environmental Science and Engineering, Tianjin University, Tianjin 300072, China*

[b] *Graduate School of Life and Environmental Sciences, University of Tsukuba, 1-1-1, Tennodai, Tsukuba, Ibaraki 305-8572, Japan*

* Corresponding author. Tel.: +81 0298-53-4655; Fax: +81 0298-53-4655.

E-mail address: songcf@iis.u-tokyo.ac.jp

Abstract

Free piston Stirling cooler (FPSC) is a promising alternative for the conventional coolers and has been applied to various fields. In the previous research, a novel cryogenic CO_2 capture system based on FPSCs has been exploited. In order to enhance the cryogenic CO_2 capture efficiency, the investigation on the coefficient of performance (COP) of the FPSC is carried out in this work. In detail, the influence of different materials (aluminium and copper), size of cold head (length and diameter), as well as ambient conditions (humidity and temperature) on the COP of the cryogenic system were tested. The experiment results indicate that the material of cold head should be selected at copper to increase the COP of CO_2 capture system. The length and diameter of cold head should be short and thick. In addition, the low ambient temperature is benefit for the high COP. For the optimal conditions (the material was copper, length and diameter were 180 and 40 mm, respectively), the temperature of the cold head reached -140 ℃, and the COP of the FPSC and the cryogenic CO_2 system was 0.82 and 0.70, respectively.

Keywords: free piston Stirling cooler, COP, performance, CO_2 capture

Nomenclature

L	Length of cold head, mm

P	Pressure, Pa
Q	Cooling capacity, J
T_a	Ambient temperature, ℃
T_c	Temperature of the cold head, ℃
V	Volume, m^3
W	Input power, J
h_a	Ambient humidity, %
m	Mass, kg
Abbreviations	
CCS	CO_2 capture and storage
COP	Coefficient of performance
FESC	Free piston Stirling cooler
LN2	Liquid nitrogen
LNG	Liquefied natural gas
PCC	Post-combustion CO_2 capture

1. Introduction

According to the prediction of Intergovernmental Panel on Climate Change (IPCC), by the year 2100, the atmosphere may contain up to 570 ppmv of CO_2, causing a rise of mean global temperature of around 1.9 ℃ and an increase in mean sea level of 3.8 m [1]. As an effective strategy to mitigating CO_2 emissions, much attention has been paid on post combustion CO_2 capture (PCC) techniques. Nowadays, the most mature post-combustion CO_2 capture technology is based on CO_2 absorption by aqueous amine solutions and has been commercially utilized on the large CO_2 emission sources (i.e. coal-fired power plants, cement and steel plant) [2,3]. In the absorption processes, CO_2 reacts reversibly in an absorber with amines which are regenerated by heating the solution in a stripper column [4]. Nevertheless, the biggest bottleneck for the chemical absorption processes is that the regeneration of solvents is energy penalty [5,6]. Meanwhile, the degradation of the aqueous amine solvents also leads to an increasing cost [7]. In light of this situation, the alternative methods (such as adsorption, membrane, cryogenic, microalgae and chemical looping) have also attracted the attention of the scientists [8]. Compared to the other CO_2 capture technologies, cryogenic CO_2 capture approach can achieve a high CO_2 purity (above 99%) and which can minimize the compression and transport costs significantly [9]. Furthermore, the CO_2 capture process can be achieved by the phase change, and there is no utilization of chemical solvents. Consequently, a number of researches have been driven toward this technique. [10-13].

As the critical part of the cryogenic CO_2 capture methods, several low temperature sources have been utilized and investigated [14]. In 2002, Clodic et al. developed a

novel cryogenic CO_2 capture process by using the cold duty from liquid nitrogen (LN2). The CO_2 in the flue gas can be recovered in the liquid form and which is beneficial to the further compression and transport. However, the main disadvantage of the process is that the deposited CO_2 on the cold head would adversely affect the heat transfer. Moreover, the moisture in the flue gas has to be separated beforehand to avoid the plugging by ice during the operation [15]. In 2011, Tuinier et al. exploited a cryogenic packed bed taking advantage of the cold energy from liquefied natural gas (LNG) regasification terminal. The moisture and CO_2 can be separated and collected at the different locations in the process. However, the coefficient of performance (COP) of the system is typically 0.5, and thus about 3.6 MJ electric energy is required and resulting in even higher thermal energy to capture per kg CO_2 [16].

Free piston Stirling cooler (FPSC) is a new type cryogenic cooler attracting interest as the low temperature source [17]. Compared to the conventional coolers, FPSC can use helium as regenerator, and avoid the increasing environmental issues (such as ozone depletion) caused by CFCs, HCFCs and HFCs [18]. Meanwhile, high energy efficiency and reliability are also the advantage of FPSC. For these reasons, FPSC has been utilized in the cryogenic CO_2 capture process in the previous work [19]. However, it needs to point out that the original cooling region of FPSC is limit duo to the size of itself. During the application process, it often needs to extend the cold head for further refrigeration. Therefore, the investigation on the COP and cryogenic temperature of FPSC is significant for improving the CO_2 capture efficiency.

The objective of this study is to investigate the characteristic of FPSC and

theoretically analyze the COP of the FPSC. The research also focuses on the influence of the key parameters on the COP of FPSC, such as the material (aluminium and copper) and size (length and diameter) of the cold head, as well as the ambient conditions (temperature and humidity). The structure of this paper is as follows. Section 2 describes the cryogenic CO_2 capture process and deduces the COP of FPSC. Section 3 shows the detailed experimental conditions. Section 4 investigates the key parameters that influence the COP and cryogenic temperature of FPSC. Section 5 discusses the possibility of increasing the efficiency by the heat exchange between the separated and incoming streams and the application in the large scale. Section 6 summarizes the main conclusions of this research.

2. Base case description

2.1. Cryogenic CO_2 capture process

The structure of designed cryogenic CO_2 capture system based on free piston Stirling coolers (FPSC) has been introduced in our previous work [20, 21]. The whole capture process can be briefly described as follows: three Stirling coolers used in the system are named as FPSC-1, FPSC-2 and FPSC-3, respectively. First, the flue gas is introduced into the pre-freezing tower. Under the low temperature, the moisture in the gas stream can condense and be separated. Then the dry flue gas flows into the main freezing tower. Under the cryogenic condition (approximately -110 ℃), the CO_2 in the gas stream frosts on the surface of the cold head of FPSC-2, and simultaneously the other gas (such as N_2 and O_2) is exhausted without phase change. Finally, the

captured CO_2 is separated by the motor driven scraper and gathered in the storage column to further compress for transport. The key parameters (such as flow rate, temperature and operating time) that affect the capture performance are controlled and recorded by the control panel.

In addition, the detailed connection of FPSC-2, cold head and main-freezing tower is shown in Fig. 1. The cold head is chilled by FPSC-2 to generate the required low temperature condition (around -110 ℃) in the main freezing tower. Therefore, during the capture process, the CO_2 in the gas stream can be separated and frosted on the surface of the cold head. It should be noted that in order to enhance the heat transfer efficiency, the vacuum interlayer is maintained between the internal of the tower and the ambient surroundings.

2.2. Free piston Stirling cooler (FPSC)

2.2.1 Theoretical analysis

A schematic diagram of the FPSC is shown in Fig. 2. The FPSC may be defined as a pressure vessel which operates by shuttling approximately 1 gram of helium back and forth by the combined movements of two parts, namely the piston and the displacer. While the piston that compresses the gas is driven by a linear motor, the displacer is moved by the pressure difference. Heat exchanger and regenerator are assembled to separate the compression and expansion spaces for the creation of a thermal gradient which allows the FPSC to extract heat from the cold head and reject heat to the region around hot head. This process is repeated many times per second

and can ultimately produce temperature differences between the cold and hot head. During the whole process, heat can be moved from a remote location to the FPSC and then rejected to the environment. The detailed working principle of FPSC has been introduced by Berchowitz in 1992 [22].

2.2.2 Coefficient of performance (COP)

As an important quality to evaluate the performance of FPSC, the investigation on the COP is significant. The COP is defined as the ratio of the cooling capacity (Q_e) and the input power (W) of the system, and can be expressed as follows:

$$COP = \frac{Q_e}{W} \tag{1}$$

where the input power (W) can be obtained from:

$$W = \frac{\omega_0}{2\pi}\int_0^{2\pi} P_c dV \tag{2}$$

here P_c and V are the pressure and volume of cylinder, and can be given by the following equations [22]:

$$P_c = \langle P \rangle + |P_c| sin\phi \tag{3}$$

$$V = V_0 - A_P X_P sin\phi \tag{4}$$

Taking equation (3) and (4) into equation (2), the input power (W) can be expressed as:

$$W = -\frac{\omega_0}{2}\alpha_T X_p X_d sin\phi \tag{5}$$

where, X_d and X_p are the amplitude of the displacer and piston. α_T is the thermal coupling between the displacer motion and piston force, and it can be calculated as follows:

$$\alpha_T = A_p \frac{\partial P_c}{\partial x_d} \tag{6}$$

In addition, the cooling capacity (Q_e) is described as follows:

$$Q_e = -\frac{\omega_0}{2}\left\{\alpha_p X_p \left(\frac{A}{A_R} - 1\right) sin\phi \; - K_{ext_d} X_p \frac{A}{A_R}\frac{m_p}{m_c} sin\phi \; + C_{ext}\omega_0 X_d \right\} X_d \tag{7}$$

where A is the crosscut area of the cylinder. C_{ext} is incidental damping. It should be noted that heat transfer losses (Q_L) is inevitable. Among the heat losses, conduction (Q_{cond}) and regenerator (H) losses are the most significant.

$$Q_L = Q_{cond} + H \tag{8}$$

In conclusion, the COP of the FPSC can be expressed as the following equation:

$$COP = \frac{\alpha_P}{\alpha_T}\left(\frac{A}{A_R} - 1\right) - \frac{A}{A_R}\frac{K_{ext}}{\alpha_T}\frac{m_P}{m_c} + \frac{C_{ext}}{\alpha_T}\frac{\omega_0}{sin\phi}\frac{X_d}{X_P} \tag{9}$$

Simultaneously, the investigation on the coefficient of performance for the whole system (COPS) is implemented to evaluate the performance of the system. The COPS of the system can be calculated as follows:

$$COPS = \frac{Q_{C1} + Q_{C2} + Q_{C3}}{W_s} \tag{10}$$

here Q_{C1}, Q_{C2} and Q_{C3} are the cooling capacity of FPSC-1, 2 and 3, respectively. W_s is the input energy of the system.

3. Experimental

The investigation of the COP are based on the experiments four parameters, namely material, length and diameter of the cold head, as well as the ambient humidity and temperature. Initially, the cold head of FPSC is tested with different materials (aluminium and copper). Then, the size (length and diameter) of the cold head is

investigated. The structure of the cold head with different materials (aluminium and copper) is shown in Fig. 3. The length (L) of cold head is set at (180 mm and 270 mm), respectively. The diameter (D) of the cold head is investigated under 30 mm and 40 mm. It needs to point out that the selection of length and diameter is just depending on the configuration of the system, and there is no special representation. Additionally, during the operating process, the FPSC needs to intake the air from ambient and exhaust the hot air simultaneously. Therefore, the influence of ambient humidity (h_a) and temperature (T_a) on the COP of FPSC is also investigated.

4. Results

4.1 Effect of the cold head on the COP

4.1.1 Material

The relationship between the COP of FPSC and the material of the cold head is investigated according with the chilling process (as shown in Fig. 4). With the temperature reduction of the cold head, the cooling capacity of FPSC decreased, and which led to the fall of COP. However, the aluminium cold head has a relative higher COP decreasing rate compared to the copper one. It results that the FPSC with an aluminium cold head has a lower COP than the copper one in the whole temperature drop process. When the root temperature of the cold head dropped to -140 ℃, the COP of FPSC with the aluminium and copper cold head are 0.61 and 0.82 respectively. It can be deduced that the COP of the copper cold head is higher than the aluminium, and which means a large cooling capacity can be obtained.

The effect of the material of cold head on the cryogenic temperature is depicted in Fig. 5. From the results, it can be concluded that the cold head made by copper has a lower temperature than aluminium. After 240 min, the root temperatures are -111.2 ℃ for the aluminium cold head and -111.3 ℃ for the copper. Meanwhile, the front temperatures of the aluminium and copper cold head are -78.09 ℃ and -97.82 ℃. In addition, the temperature decreasing rate for the copper cold head is higher than the aluminium. For copper, the temperature drop from the root of the cold head to the front is 13.38 ℃. By contrast, although the mass of the cold head by aluminium is light, the thermal loss is great (with a temperature drop of 33.31 ℃).

4.1.2 Length

The results in Fig. 6 show that the influence of the length of cold head on the COP of FPSC. It can be observed that with the increase of the length, the COP of FPSC decreased obviously. However, for the aluminium cold head, the decreasing rate of COP is higher than the copper one. When the length is extended from 180 mm to 270 mm, the COP dropped from 0.82 down to 0.59 (the root temperature of the cold head was -140 ℃). It can be explained by the fact that along with the increasing of the length of the cold head, the heat loss also increase and the cooling capacity of the cold head reduced accordingly. Therefore, the COP of FPSC also dropped.

As the results in Fig. 7, the cryogenic temperature of the cold head decreases with the extension of the length. When the length of the cold head is set at 180 mm, the temperature drop from the root to the front is 9.92 ℃. However, with the length

extending to 270 mm, the temperature drop rose up to 15.73 ℃. Furthermore, after 240 min, the front temperature of the cold head for 180 mm and 270 mm are -84.08 ℃ and -73.17 ℃. That is because that along with the extension of the length, the temperature loss of the cold head also increases.

4.1.3 Diameter

As presented in Fig. 8, the COP variation process with different diameters was investigated. The COP of FPSC reduced according with the temperature drop of the cold head. With the expanding of the diameter of the cold head (from 30 mm to 40 mm), the COP of FPSC increased obviously. Meanwhile, the decreasing rate of the COP was decelerated. When the root temperature of the cold head decreased to -140 ℃, the COP was 0.52 (diameter of 30mm) and 0.59 (diameter of 40 mm), respectively.

In addition, the relationship between the diameter and cryogenic temperature of the cold head was depicted in Fig. 9. From the results, it can be concluded that a large diameter is beneficial to reduce temperature loss. When the diameter of the cold head is set at 30 mm, the lowest temperature for the root and front of the cold head is -85 ℃ and -64.72 ℃. The temperature drop is 20.28 ℃ from the root to the front side. By contrast, when the diameter is set at 40 mm, the lowest temperature for the root and front sides is -88.9 ℃ and -73.17 ℃ respectively. The temperature drop can be reduced to 15.73 ℃. For the larger diameter (40 mm), both of the root and front temperature are lower than the smaller one (30 mm). It indicated that expanding the

diameter of the cold head is beneficial to improve heat transfer efficiency and the COP of FPSC.

4.2 Effect of the ambient conditions on the COP

The effect of ambient temperature on the COP of FPSC is summarized in Fig. 10. From the result, it can be observed that the COP of FPSC increased with the decreasing of ambient temperature. When the ambient temperature varied from 8 ℃ to 28 ℃, the COP of FPSC reduced from 0.7 to 0.6. That is for the reason that during the refrigeration process of FPSC, it absorbs cool air from surrounding and simultaneously exhausts warm air. A low ambient temperature is favor of increasing temperature difference from the cold head of FPSC to the warm side. Thus, in order to improve the performance of FPSC, the ambient temperature should be dropped as low as possible. The influence of ambient humidity on the COP of FPSC is shown in Fig. 11. From the results in the figure, it shows that with the ambient humidity increasing from 20 % to 75 %, the COP of FPSC varied in the range of 0.62 to 0.68. It indicated that the influence of ambient humidity on the COP of FPSC is not significant.

4.3 COP of the cryogenic CO_2 capture system

The COP variation of the FPSCs (FPSC-1, 2 and 3) and the whole system is shown in Fig. 12. From the results, it can be found that the COPs of three FPSCs were different. That is for the reason that due to the different functions in the cryogenic CO_2 capture system, the length of the cold head of the FPSCs is also different. When the temperature of the cold head for FPSC-2 was cooled to -140 ℃, the COPs of

FPSC-1, 2 and 3 were 0.82, 0.78 and 0.79, respectively. Meanwhile, due to the other energy consumption units (such as vacuum pump, control panel and scraper), the COP of the whole system was 0.70.

5. Discussion

The COP of the Stirling cooler and the developed cryogenic CO_2 capture system has been tested under various conditions (including material, length and diameter of the cold head, as well as the ambient temperature and humidity) to achieve the optimal performance of the system. Simultaneously, the temperature of the cold head was also investigated to evaluate the cryogenic performance of the Stirling cooler. It can be concluded that the COP of the Stirling cooler is higher (about 0.82 at -140 ℃) than the common refrigerators (around 0.5 at -140 ℃).

Although the cryogenic CO_2 capture process has several advantages, it still suffers some limitations need to be overcome. It should be noticed that the whole capture process is based on the low temperature condition, and thus the latent heat associated with the separated components (i.e. the condensate water, exhaust gas and especially captured CO_2) would be substantial. For the future work, the cold energy of these components should be recovered by the heat exchangers, and then the total energy consumption of the system could be further reduced.

Owing to the flow rate of flue gas in the real power plants is higher than the laboratory scale, the scaling up of the capture capacity of the system is very significant. It can be achieved by utilizing the high power Stirling coolers. Meanwhile,

more Stirling coolers can be integrated into the system to improve the chilling ability of each parts (such as pre-freezing, main freezing and storage towers). However, it should be pointed out that with the increase of the amount of the Stirling coolers, the phenomenon of oscillation of the system may become increasing serious. Therefore, the influence of the oscillation phenomenon on the COP of Stirling cooler should be studied in the future research.

6. Conclusion

In the present work, the investigation on the COP of the FPSC was carried out. In order to improve the COP of FPSC in the cryogenic CO_2 capture process, the key parameters (material, length and diameter of the cold head, as well as the ambient temperature and humidity) were also investigated. Based on the experimental results, the conclusions are summarized as follows:

1) From the experiment of the materials, it can be concluded that when the cold head was made by copper, the COP of FPSC was 0.82 with -140 ℃ of the cold head. By contrast, the COP of FPSC for the aluminium cold head was 0.61.

2) For the different lengths of the cold head (270 mm and 180 mm), the COP of FPSC was 0.59 and 0.82, respectively. Furthermore, when the diameter of the cold head was set at 30 mm, the COP of FPSC was 0.52. By contrast, with the diameter thickening to 40 mm, the COP of FPSC increased to 0.59.

3) In addition, the ambient temperature also presented a significant influence on the COP of FPSC. When the ambient temperature varied from 8 ℃ to 28 ℃, the COP of

FPSC reduced from 0.7 to 0.6. Nevertheless, the effect of ambient humidity on the COP is not significant. With the ambient humidity increasing from 20 % to 75 %, the COP of FPSC varied in the range of 0.62 to 0.68.

4) Although the FPSCs in the system had high COPs, the COP of the system was around 0.70 due to other energy consumption units (such as vacuum pump and control panel).

Acknowledgement

We thank Mr. Yamano and Mr. Yamasaki of Tanabe Engineering Corporation for their technological assistance.

References

[1] IPCC. Summary for policymakers. In: climate change 2007: the physical science basis, contribution of working group I to the fourth assessment report of the intergovernmental panel on climate change. Geneva: World Meteoro-logical Organization/United Nations Environment Program; 2007.

[2] Abu-Zahra MRM, Schneiders LHJ, Niederer JPM, Feron PHM, Versteeg GF. CO_2 capture from power plants Part I. A parametric study of the technical performance based on monoethanolamine. Int. J. Greenhouse Gas Control 2007;1:37-46.

[3] Versteeg P, Rubin ES. A technical and economic assessment of ammonia-based post-combustion CO_2 capture at coal-fired power plants. Int. J. Greenhouse Gas Control. 2011;5:1596-1605.

322 [4] Gouedard C, Picq D, Launay F, Carrette PL. Amine degradation in CO_2 capture. I. A review.
323 Int. J. Greenhouse Gas Control. 2012;10:244-270.
324 [5] Luis P, Gerven TV, Bruggen BV. Recent developments in membrane-based technologies for
325 CO_2 capture. Progress in Energy and Combustion Science. 2012;38:419-448.
326 [6] Lee ZH, Lee KT, Bhatia S, Mohamed AR. Post-combustion carbon dioxide capture: Evolution
327 towards utilization of nanomaterials. Renewable & Sustainable Energy Reviews
328 2012;16:2599-2609.
329 [7] Dumée L, Scholes C, Stevens G, Kentish S. Purification of aqueous amine solvents used in
330 post combustion CO_2 capture: A review. Int. J. Greenhouse Gas Control 2012;10:443-455.
331 [8] Rubin ES, Mantripragada H, Marks A, Versteeg P, Kitchin J. The outlook for improved carbon
332 capture technology. Progress in Energy and Combustion Science 2012;38:630-671.
333 [9] Belaissaoui B, Moullec YL, Willson D, Favre E. Hybrid membrane cryogenic process for
334 post-combustion CO_2 capture. J. Membrane Sci 2012;415-416:424-434.
335 [10] Clodic D, Younes M, Bill A. Test results of CO_2 capture by anti-sublimation Capture
336 efficiency and energy consumption for Boiler plants. Seventh International Conference on
337 Greenhouse Gas control Technologies GHGT7, Vancouver, Canada, 6-9 September 2004
338 [11] Tuinier MJ, vanSintAnnaland M, Kramer GJ, Kuipers JAM. Cryogenic CO_2 capture using
339 dynamically operated packed beds. Chem Eng Sci. 2010;65:114-119.
340 [12] Swanson CE, Elzey JW, Hershberger RE, Donnelly RJ. Thermodynamic analysis of
341 low-temperature carbon dioxide and sulfur dioxide capture from coal-burning power plants.
342 Physical Review E 2012;86:016103.

[13] Lively RP, Koros WJ, Johnson JR. Enhanced cryogenic CO_2 capture using dynamically operated low-cost fiber beds. Chem Eng Sci 2012;71:97-103.

[14] Berstad D, Anantharaman R, Neksa P. Low-temperature CO_2 capture technologies - Applications and potential. Int. J. Refrigeration 2013;36:1403-1416.

[15] Clodic D, Younes M. A new method for CO_2 capture: frosting CO_2 at atmospheric pressure. Sixth International Conference on Greenhouse Gas Control Technologies, GHGT-6, Kyoto, Japan, 1-4 October, 2002. pp.155-160.

[16] Tuinier, M.J., van Sint Annaland, M., Kuipers, J.A.M.. A novel process for cryogenic CO_2 capture using dynamically operated packed beds—An experimental and numerical study. Int J Greenh Gas Con. 2011;5:694-701.

[17] Berchowitz DM, Kiikka D, Mennink BD. Recent advances in Stirling cycle refrigeration. 19th International Congress on Refrigeration Exhibition. August 20-25, 1995, the Hague, the Netherlands.

[18] Mennink BD, Goossen WJ. The free-piston Stirling cooling system improving the energy efficiency of refrigerators. 19th International Congress on Refrigeration Exhibition. August 20-25, 1995, The Hague, The Netherlands.

[19] Song CF, Kitamura Y, Li SH, Ogasawara KJ. Design of a cryogenic CO_2 capture system based on Stirling coolers. Int. J. Greenhouse Gas Control. 2012;7:107-114.

[20] Song CF, Kitamura Y, Li SH, Jiang WZ. Parametric analysis of a novel cryogenic CO_2 capture system based on Stirling coolers. Environ. Sci. Technol 2012;46(22):12735–12741.

[21] Song CF, Kitamura Y, Li SH. Evaluation of Stirling cooler system for cryogenic CO_2 capture. Applied Energy 2012;98:491-501.

[22] Berchowitz, DM. Free-Piston Stirling Coolers (1992). International Refrigeration and Air Conditioning Conference. Paper 171. http://docs.lib.purdue.edu/iracc/171.

Figure captions:

Fig. 1. The detailed connection of FPSC-2, cold head and main-freezing tower. (The gray area represents the vacuum condition of the interlayer in the system.)

Fig. 2. The detailed configuration of FPSC.

Fig. 3. The cold head of FPSC with different materials (aluminium and copper).

Fig. 4. COP variation of FPSC with the root temperature of the cold head under different material (L=180 mm; D=40 mm).

Fig. 5. The effect of the material of cold head on the cryogenic temperature (L=180 mm; D=40 mm).

Fig. 6. COP variation of FPSC with the root temperature of cold head under different length (L) (material of cold head is copper; D=40 mm).

Fig. 7. The relationship of length (L) and cryogenic temperature (T_c) of the cold head (material of cold head is copper; D=40 mm).

Fig. 8. COP variation of FPSC with the root temperature of cold head under different diameter (D) (material of cold head is copper; L=270 mm).

Fig. 9. The relationship of diameter (D) and cryogenic temperature (T_c) of the cold head (material of cold head is copper; L=270 mm).

Fig. 10. COP variation of FPSC with the different ambient temperature (T_a) (material of cold head is copper; L=180 mm; D=40 mm).

Fig. 11. COP variation of FPSC with different ambient humidity (h_a) (material of cold head is copper; L=180 mm; D=40 mm).

Fig. 12. COP variation of the FPSCs and system with the root temperature of FPSC-2's cold head (material of cold head is copper; L=180 mm; D=40 mm). COP-1, COP-2, COP-3 and COPS represent the coefficient of performance for FPSC-1, FPSC-2, FPSC-3 and the whole system, respectively.

405

406

407

408

409

410

411

412

413

414

415

416

417

418

419

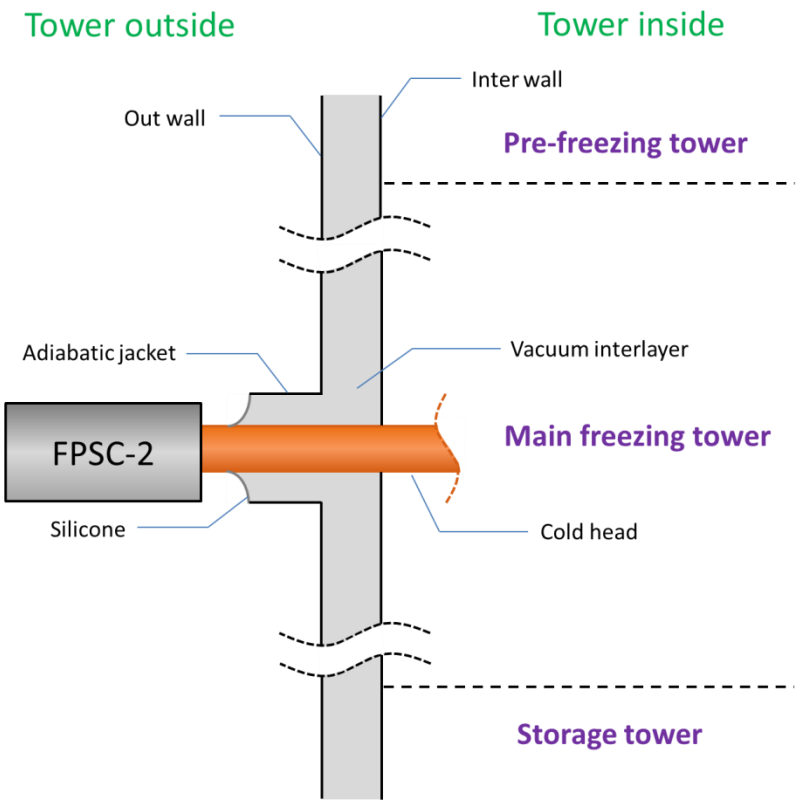

Fig. 1. The detailed connection of FPSC-2, cold head and main-freezing tower. (The gray area represents the vacuum condition of the interlayer in the system.)

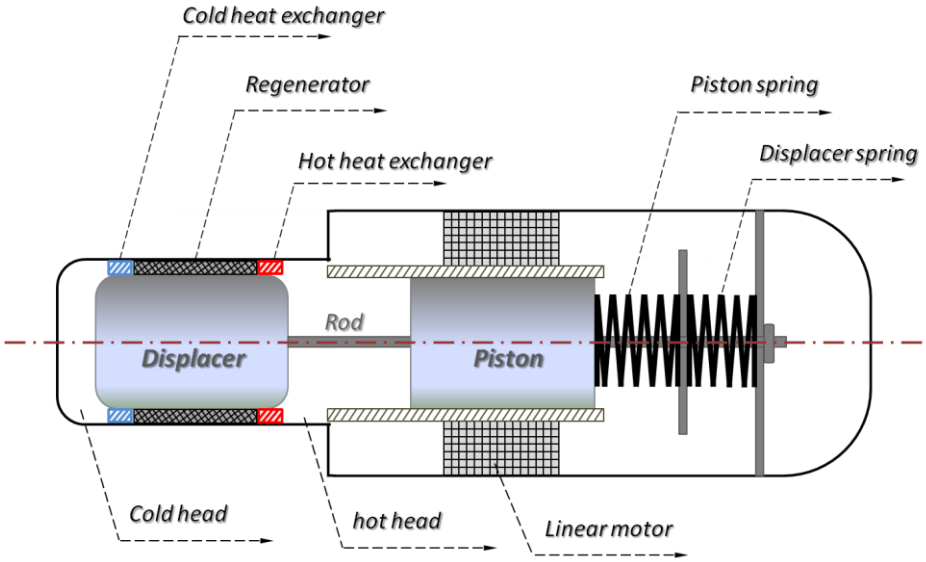

Fig. 2. The detailed configuration of FPSC.

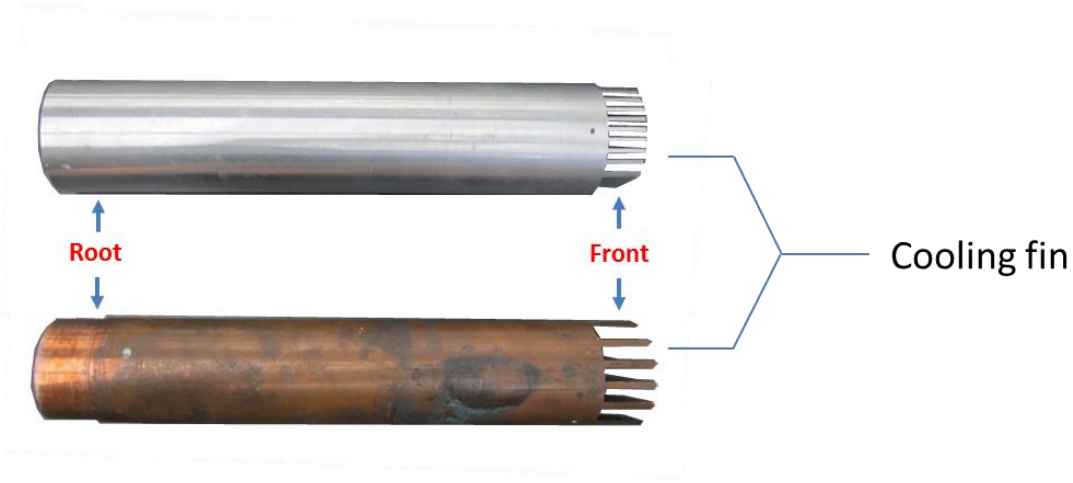

Fig. 3. The cold head of FPSC with different materials (aluminium and copper).

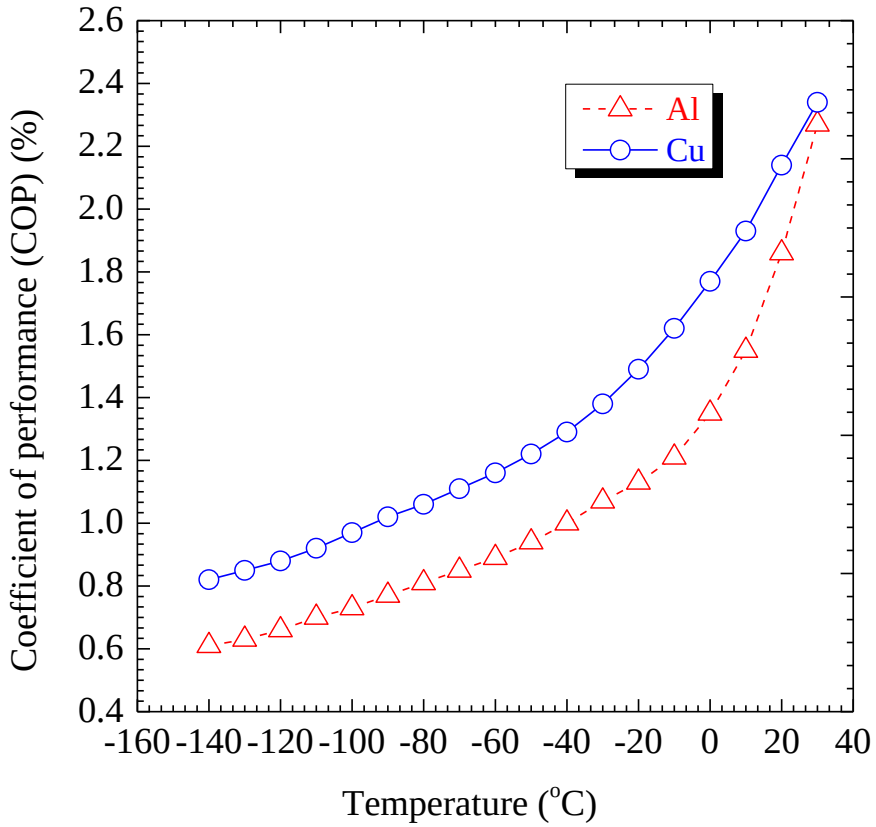

Fig. 4. COP variation of FPSC with the root temperature of the cold head under different material (L=180 mm; D=40 mm).

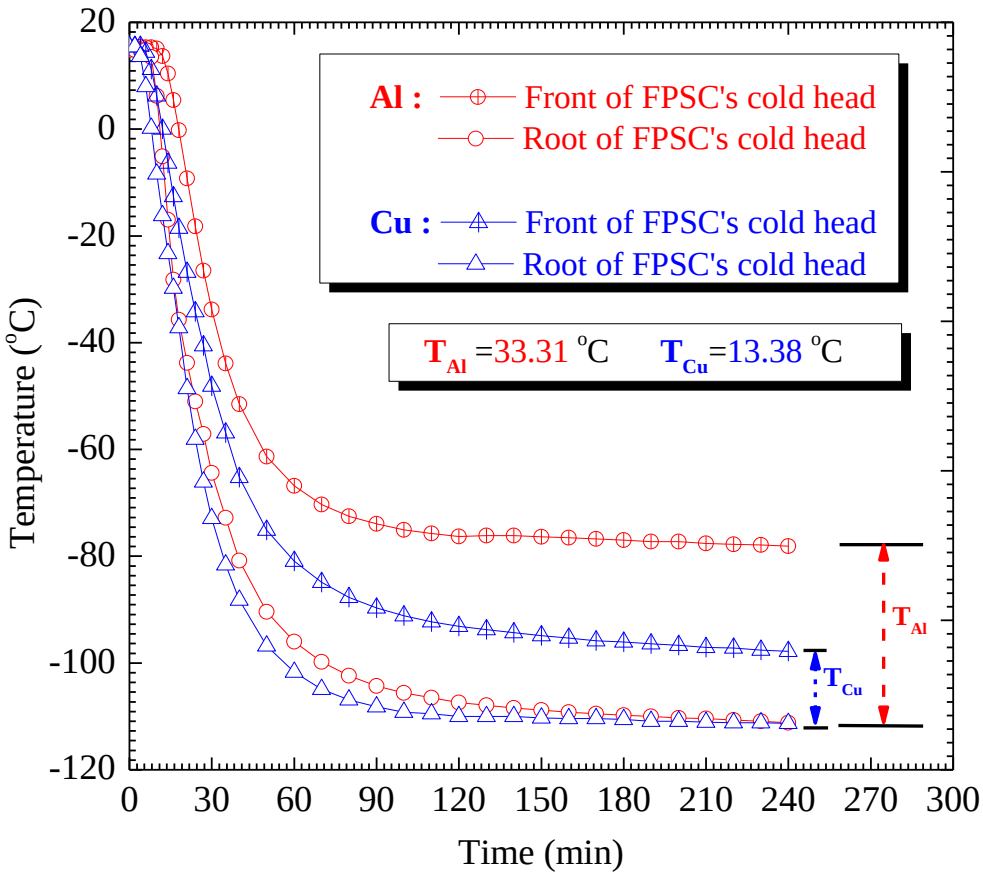

Fig. 5. The effect of the material of cold head on the cryogenic temperature (L=180 mm; D=40 mm).

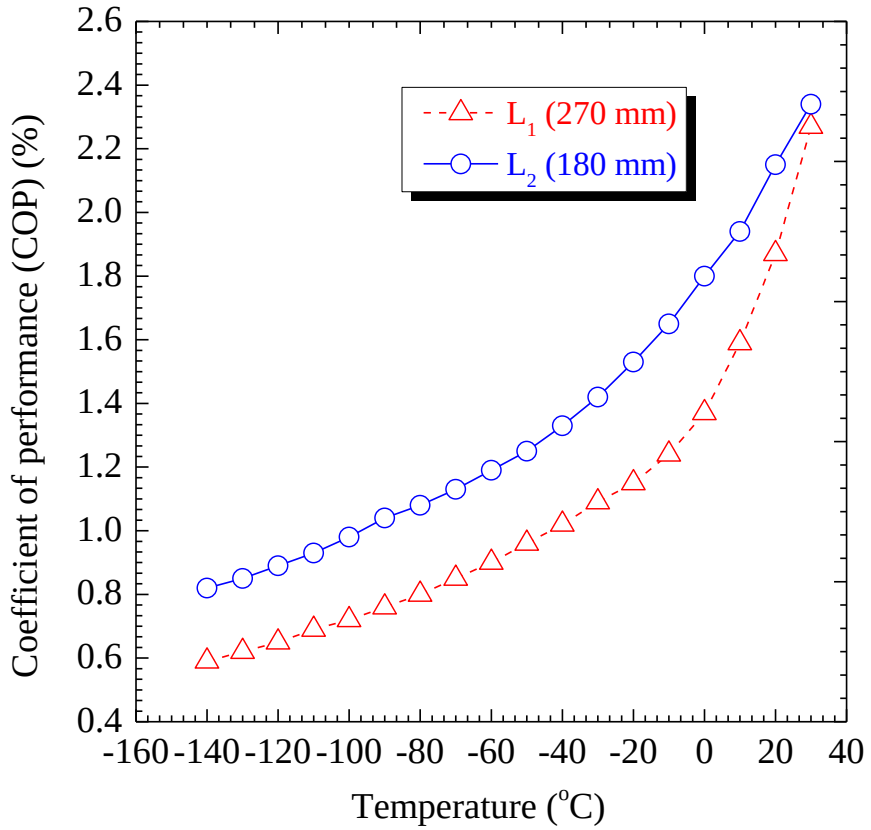

Fig. 6. COP variation of FPSC with the root temperature of cold head under different length (*L*) (material of cold head is copper; *D*=40 mm).

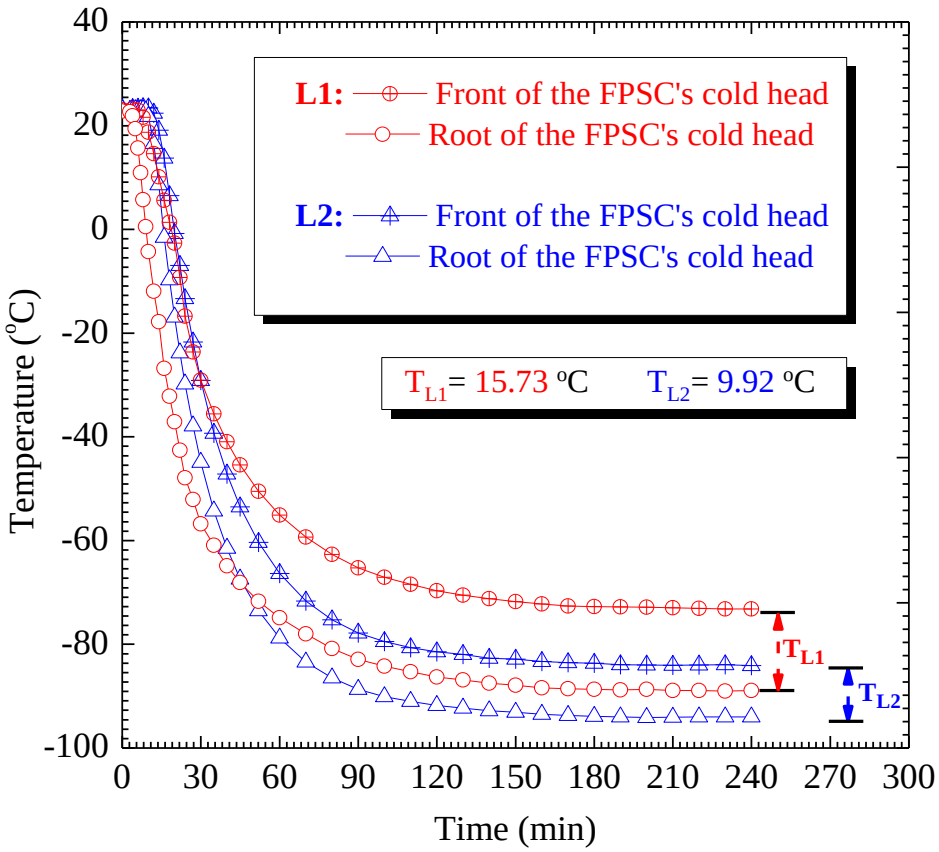
L1: Front of the FPSC's cold head
Root of the FPSC's cold head
L2: Front of the FPSC's cold head
Root of the FPSC's cold head
T_L1= 15.73 ºC
T_L2= 9.92 ºC
ΔT_L1
ΔT_L2
Temperature (ºC)
Time (min)
40
20
0
-20
-40
-60
-80
-100
0
30
60
90
120
150
180
210
240
270
300

Fig. 7. The relationship of length (L) and cryogenic temperature (T_c) of the cold head (material of cold head is copper; D=40 mm).

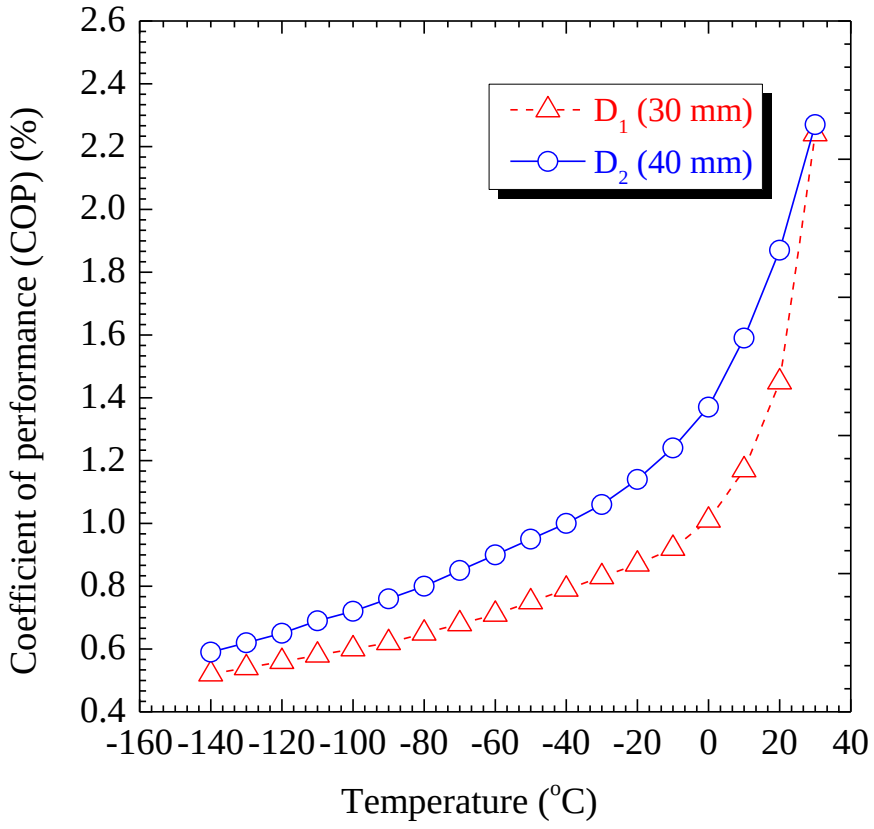

507

508

509 **Fig. 8.** COP variation of FPSC with the root temperature of cold head under different diameter (*D*)

510 (material of cold head is copper; *L*=270 mm).

511

512

513

514

515

516

517

518

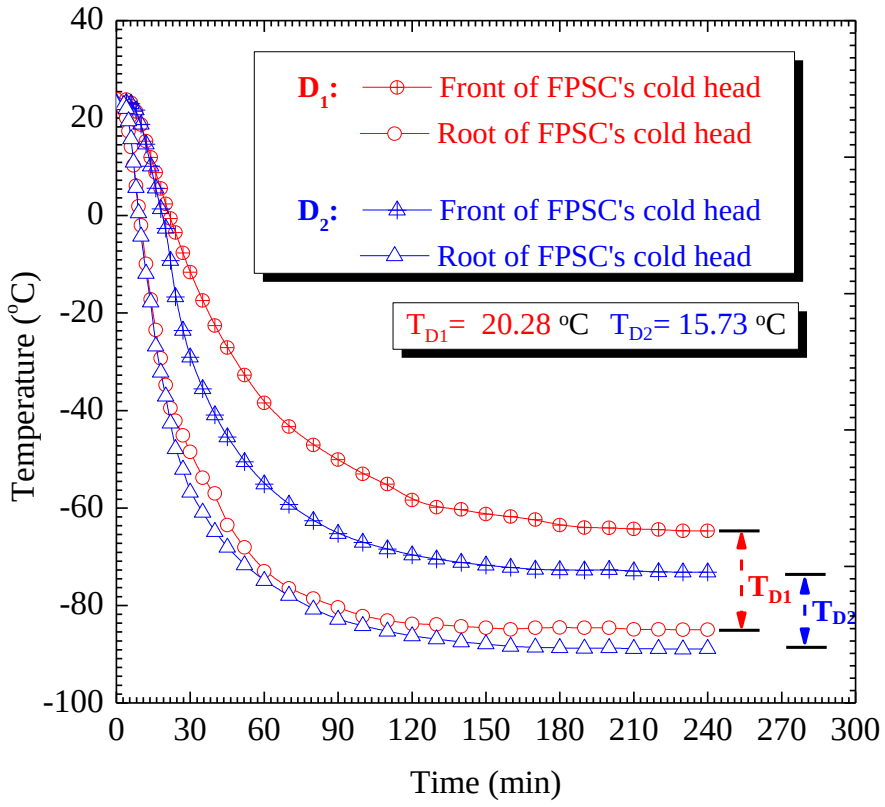

Fig. 9. The relationship of diameter (D) and cryogenic temperature (T_c) of the cold head (material of cold head is copper; L=270 mm).

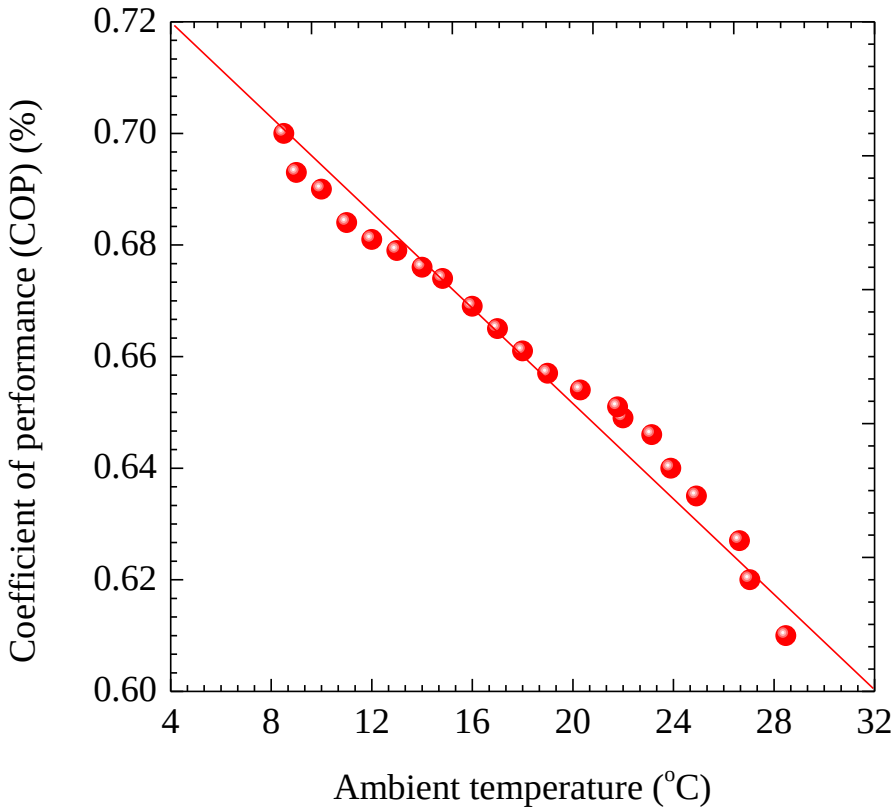

Fig. 10. COP variation of FPSC with the different ambient temperature (T_a) (material of cold head is copper; L=180 mm; D=40 mm).

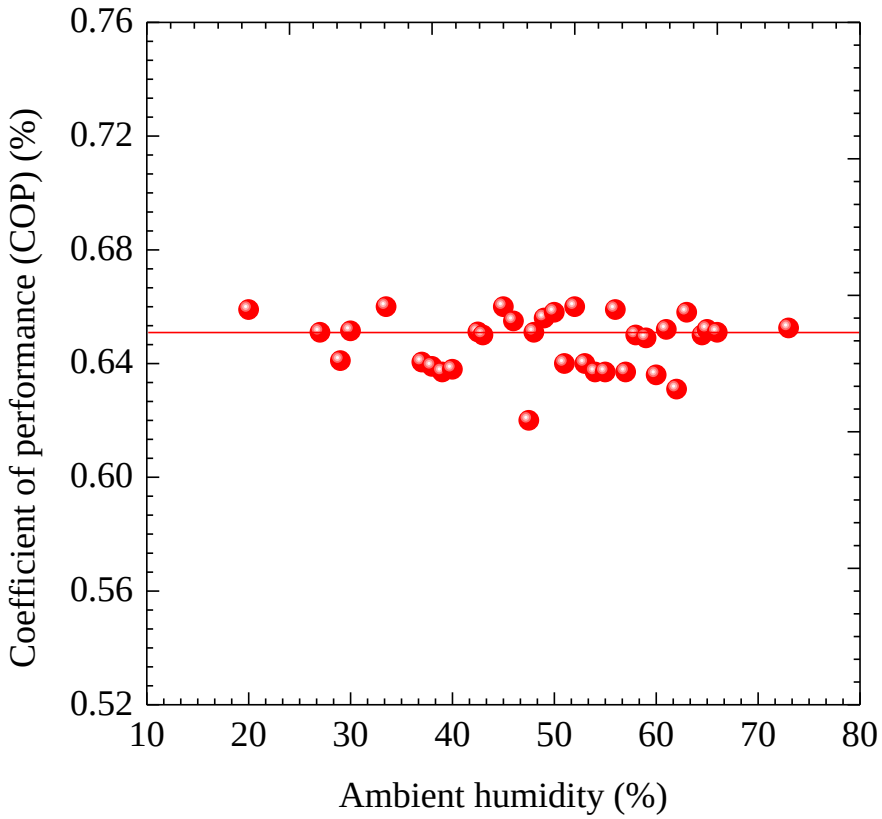

Fig. 11. COP variation of FPSC with different ambient humidity (h_a) (material of cold head is copper; L=180 mm; D=40 mm).

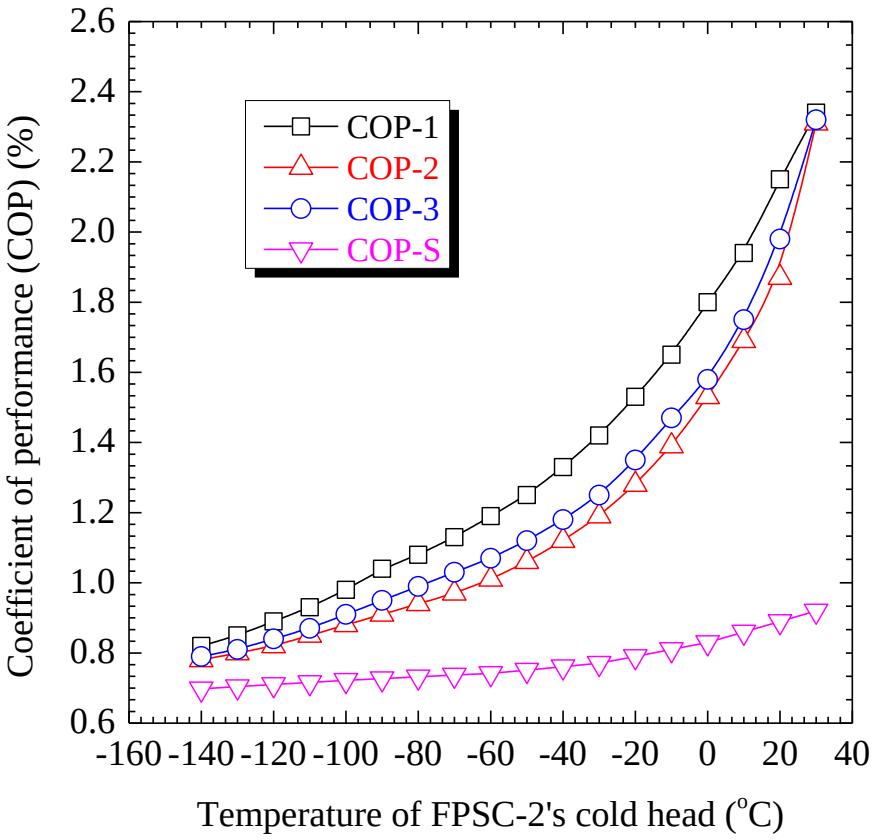

Fig. 12. COP variation of the FPSCs and system with the root temperature of FPSC-2's cold head (material of cold head is copper; L=180 mm; D=40 mm). COP-1, COP-2, COP-3 and COPS represent the coefficient of performance for FPSC-1, FPSC-2, FPSC-3 and the whole system, respectively.

571